



Research Article

FREE TRANSVERSE VIBRATIONS OF ROTATING ANNULAR DISKS UNDER VARIOUS BOUNDARY CONDITIONS

Mertol TUFEKCI*¹, Hilal KOC², Omer Ekim GENEL³, Olcay OLDAC⁴

¹Istanbul Technical University, Faculty of Mechanical Engineering, Gumussuyu-ISTANBUL;
ORCID:0000-0002-5530-1471

²Istanbul Technical University, Faculty of Mechanical Engineering, Gumussuyu-ISTANBUL;
ORCID:0000-0002-9655-0298

³Istanbul Technical University, Faculty of Mechanical Engineering, Gumussuyu-ISTANBUL;
ORCID:0000-0003-2574-5036

⁴Istanbul Technical University, Faculty of Mechanical Engineering, Gumussuyu-ISTANBUL;
ORCID:0000-0003-1292-7092

Received: 02.02.2018 Revised: 23.07.2018 Accepted: 30.08.2018

ABSTRACT

Free vibrations of rotating disks are investigated by using the Galerkin method. An approximate function which satisfies the boundary conditions and normalizing constraint is chosen. The different boundary conditions are also investigated in order to understand the vibrational characteristics of this type of structures. The stress distributions on the rotating disk with different boundary conditions are used in the analysis. The effects of rotation speed on the natural frequencies are studied. The results are presented in tables and figures and also compared with the results given in the literature.

Keywords: Rotating annular disk, Free vibrations, Galerkin method.

1. INTRODUCTION

Studies on stationary and rotating disks date back to the beginning of the twentieth century. The advances in technology have led to a vast field of research on vibrations occurring in disks rotating at higher speeds. Turbines, high-speed fans, gears, train wheels, saw blades are some examples to be given as the application of spinning disks. For example, the problem of noise from the brake disk, one of the current topics in the automotive industry, is closely related to the vibrations of rotating disks. In recent years, it has been observed that studies related to rotating disks are directed towards the information storage industry. Contact between the read/write head and the disk can be affected by vibrations due to the disk rotation, especially since the hard disks rotate at very high speeds and this interaction can cause a severe failure on the hard disk surface. The first studies of the vibrations of rotating disks were performed by Lamb and Southwell [1]. Southwell [2] utilized the linear theory and neglected the bending stiffness. The first study on nonlinear vibrations of rotating disks is presented by Nowinski [3]. Mote [4] used the Rayleigh-Ritz method for disks with varying thickness, clamped at inner and free at outer circumferences.

* Corresponding Author: e-mail: tufekcime@itu.edu.tr, tel: (212) 293 13 00 / 2489

Ramaiah [5] and Bashmal [6] used the same method for various boundary conditions. In [6], Bashmal et al. benefited from this method to investigate vibrations of stationary disks. In addition, Koo [7] also used the Rayleigh-Ritz method to obtain the natural frequencies of composite disks. In addition to the Rayleigh-Ritz method, which is a variational approach, the natural frequencies of rotating disks were investigated by using the Galerkin method. Pei and Tan [8] used the Galerkin method to study the modal interactions in rotating disks. In recent years, Mignolet et al. [9] used perturbation techniques to investigate the free vibrations of disks with and without hole at the center. Nayfeh et al. [10] investigated both linear and nonlinear vibrations using a multi scale approach.

In this study, the Galerkin method is used to determine the free vibration characteristics of rotating disks. In this method, an approximate function which satisfies the boundary conditions of the disk is selected and substituted in the differential equation of motion. Free vibrations of rotating disks with various boundary conditions are also investigated. The results are compared with those given in literature.

2. ANALYSIS

The differential equation of a rotating disk with rotation speed Ω , that is written in the coordinates (r, φ) attached to the disk, has the following form;

$$D \left(\frac{\partial^2}{\partial r^2} + \frac{1}{r} \frac{\partial}{\partial r} + \frac{1}{r^2} \frac{\partial^2}{\partial \varphi^2} \right)^2 w + \rho h \frac{\partial^2 w}{\partial t^2} - \frac{h}{r} \left[\frac{\partial}{\partial r} \left(\sigma_r r \frac{\partial w}{\partial r} \right) + \frac{1}{r} \sigma_\varphi \frac{\partial^2 w}{\partial \varphi^2} \right] = 0 \quad (1)$$

Here, w is the transverse displacement of the disk, h is the disk thickness, $D = Eh^3/[12(1 - \nu^2)]$ is the bending stiffness of the disk, (r, φ) the coordinates fixed to disk, t is the time, ρ is the density of the disk material, σ_r and σ_φ are the radial and tangential stresses due to the rotation of the disk and these stresses depend on the boundary conditions of the disk.

The transverse displacement function has the form as follows;

$$w = \sum_{n=0}^N \sum_{m=0}^M a_{mn} R_{mn}(r) \sin[n\varphi + (n\Omega - \omega)t] \quad (2)$$

Galerkin method is used for the solution. The approximate function $R_{mn}(r)$ which satisfies the boundary conditions is chosen as follows;

$$R_{mn}(r) = X_{mn}^1 r^m + X_{mn}^2 r^{m+1} + X_{mn}^3 r^{m+2} + X_{mn}^4 r^{m+3} + X_{mn}^5 r^{m+4} \quad (3)$$

$X_{mn}^1, X_{mn}^2, X_{mn}^3, X_{mn}^4$ and X_{mn}^5 are unknown constants and determined using the boundary conditions and the normalizing constraint of the disk.

If $R_{mn}(r)$ is substituted in Equation (2) and then Equation (1), the following is obtained.

$$\sum_{n=0}^M \sum_{m=0}^N \left\{ D \left(\frac{\partial^4}{\partial r^4} + \frac{2}{r} \frac{\partial^3}{\partial r^3} - \frac{2n^2+1}{r^2} \frac{\partial^2}{\partial r^2} + \frac{2n^2+1}{r^3} \frac{\partial}{\partial r} + \frac{n^4-4n^2}{r^4} \right) R_{mn}(r) - \rho h (n\Omega - \omega)^2 R_{mn}(r) - \frac{h}{r} \left[\frac{d}{dr} \left(\sigma_r r \frac{dR_{mn}(r)}{dr} \right) - \frac{n^2}{r} \sigma_\varphi R_{mn}(r) \right] \right\} \cdot a_{mn} \cdot \sin[n\varphi + (n\Omega - \omega)t] = 0 \quad (4)$$

Here, for each value of n , the term, $\sin[n\varphi + (n\Omega - \omega)t]$ does not have to be equal to zero. In order to satisfy this equation, the term in the braces has to be equal to zero:

$$\left\{ D \left(\frac{\partial^4}{\partial r^4} + \frac{2}{r} \frac{\partial^3}{\partial r^3} - \frac{2n^2+1}{r^2} \frac{\partial^2}{\partial r^2} + \frac{2n^2+1}{r^3} \frac{\partial}{\partial r} + \frac{n^4-4n^2}{r^4} \right) R_{mn}(r) - \rho h (n\Omega - \omega)^2 R_{mn}(r) - \frac{h}{r} \left[\frac{d}{dr} \left(\sigma_r r \frac{dR_{mn}(r)}{dr} \right) - \frac{n^2}{r} \sigma_\varphi R_{mn}(r) \right] \right\} \cdot a_{mn} = 0 \quad (5)$$

This is the residual and the weighted residual has to be equal to zero.

$$\int_0^{2\pi} \int_{R_i}^{R_o} \sum_{n=0}^N \sum_{m=0}^M \left\{ D \left(\frac{\partial^4 R_{mn}(r)}{\partial r^4} + \frac{2}{r} \frac{\partial^3 R_{mn}(r)}{\partial r^3} - \frac{2n^2+1}{r^2} \frac{\partial^2 R_{mn}(r)}{\partial r^2} + \frac{2n^2+1}{r^3} \frac{\partial R_{mn}(r)}{\partial r} + \frac{n^4-4n^2}{r^4} R_{mn}(r) \right) - \rho h (n\Omega - \omega)^2 R_{mn}(r) - \frac{h}{r} \left[\sigma_r r \frac{\partial^2 R_{mn}(r)}{\partial r^2} + \left(\frac{\partial \sigma_r}{\partial r} r + \sigma_r \right) \frac{\partial R_{mn}(r)}{\partial r} - \frac{n^2}{r} \sigma_\phi R_{mn}(r) \right] \right\} a_{mn} a_{sn} R_{sn}(r) \sin[n\phi + (n\Omega - \omega)t] r dr d\phi = 0 \tag{6}$$

where $s = 0, 1, 2, \dots, M$.

Here, only the sine function is dependent of ϕ . Therefore, the integral of this expression does not have to be equal to zero. Rearranging this expression will give the following:

$$\sum_{n=0}^N \sum_{m=0}^M \left\{ \frac{1}{\rho h} \int_{R_i}^{R_o} D \left(\frac{\partial^4 R_{mn}(r)}{\partial r^4} + \frac{2}{r} \frac{\partial^3 R_{mn}(r)}{\partial r^3} - \frac{2n^2+1}{r^2} \frac{\partial^2 R_{mn}(r)}{\partial r^2} + \frac{2n^2+1}{r^3} \frac{\partial R_{mn}(r)}{\partial r} + \frac{n^4-4n^2}{r^4} R_{mn}(r) \right) R_{sn}(r) r dr - \frac{1}{\rho h} \int_{R_i}^{R_o} h \left[\sigma_r r \frac{\partial^2 R_{mn}(r)}{\partial r^2} + \left(\frac{\partial \sigma_r}{\partial r} r + \sigma_r \right) \frac{\partial R_{mn}(r)}{\partial r} - \frac{n^2}{r} \sigma_\phi R_{mn}(r) \right] R_{sn}(r) dr - (n\Omega - \omega)^2 \int_{R_i}^{R_o} R_{mn}(r) R_{sn}(r) r dr \right\} a_{mn} a_{sn} = 0 \tag{7}$$

The following definitions can be used:

$$\begin{aligned} \phi_{smn} &= \frac{1}{\rho h} \int_{R_i}^{R_o} D \left(\frac{d^4 R_{mn}(r)}{dr^4} + \frac{2}{r} \frac{d^3 R_{mn}(r)}{dr^3} - \frac{2n^2+1}{r^2} \frac{d^2 R_{mn}(r)}{dr^2} + \frac{2n^2+1}{r^3} \frac{dR_{mn}(r)}{dr} + \frac{n^4-4n^2}{r^4} R_{mn}(r) \right) R_{sn}(r) r dr - \\ &\frac{1}{\rho h} \int_{R_i}^{R_o} h \left[\sigma_r r \frac{d^2 R_{mn}(r)}{dr^2} + \left(\frac{\partial \sigma_r}{\partial r} r + \sigma_r \right) \frac{dR_{mn}(r)}{dr} - \frac{n^2}{r} \sigma_\phi R_{mn}(r) \right] R_{sn}(r) dr \end{aligned} \tag{8}$$

$$\Gamma_{smn} = \int_{R_i}^{R_o} R_{mn}(r) R_{sn}(r) r dr \tag{9}$$

$$\lambda_{mn} = (n\Omega - \omega) \tag{10}$$

$$A_{smn} = a_{mn} a_{sn} \tag{11}$$

If the terms, λ_{mn} , ϕ_{smn} and Γ_{smn} are used, Equation (7) can be rewritten as follows;

$$\sum_{n=0}^N \sum_{m=0}^M [\phi_{smn} - \lambda_{mn}^2 \Gamma_{smn}] A_{smn} = 0 \tag{12}$$

For each value of n , this sum gives a linear system of equations in terms of the unknown coefficients A_{smn} . In order to solve the linear systems of equations, for each value of n , the determinant of coefficient matrix in Equation (12) must be zero and this gives a polynomial in terms of λ_{mn}^2 . The roots λ_{mn}^2 are obtained then natural frequencies of rotating disks can be calculated as follows;

$$\omega_{mn1,2} = n\Omega \pm \lambda_{mn} \tag{13}$$

As can be seen from this equation, there is only one frequency value for a non-rotating disk for each (m, n) value. In the case of rotating disk, in all modes, the frequency is divided into two different values except for $n=0$ modes, as frequencies of forward and backward traveling waves.

In order to obtain the frequency, $R_{mn}(r)$ function has to be determined. Therefore, the boundary conditions of the disk will be utilized, and the constants $X_{mn}^1, X_{mn}^2, X_{mn}^3, X_{mn}^4$ and X_{mn}^5 can be determined easily. In this study, clamped-clamped, clamped-free, free-free and free-clamped boundary conditions are considered. Figure 1 shows all investigated boundary conditions.

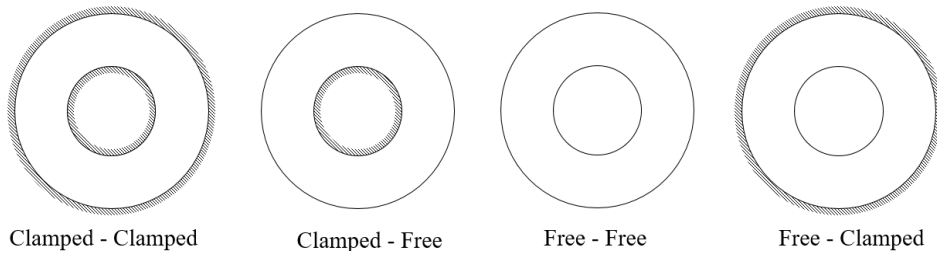


Figure 1. Investigated boundary conditions.

The stress distributions of clamped-clamped boundary conditions are given as follows:

$$\sigma_r = \frac{\rho\Omega^2}{8} \left[(1 + \nu)(R_i^2 + R_o^2) - \frac{(1-\nu)R_i^2R_o^2}{r^2} - (1 + 3\nu)r^2 \right] \quad (14)$$

$$\sigma_\varphi = \frac{\rho\Omega^2}{8} \left[R_o^2 \left(1 - \frac{R_i^2}{r^2} \right) + \nu R_i^2 \left(1 + \frac{R_o^2}{r^2} \right) - (1 + 3\nu)r^2 \right] \quad (15)$$

Stress distributions in rotating disk with clamped-free boundary conditions are given in the following equation;

$$\sigma_r = \frac{(3+\nu)}{8} \rho\Omega^2 (R_o^2 - r^2) + \frac{\rho\Omega^2 R_i^2 (1-\nu) [R_o^2 (3+\nu) - R_i^2 (1+\nu)]}{8 [R_i^2 (1-\nu) + R_o^2 (1+\nu)]} \left(\frac{R_o^2}{r^2} - 1 \right) \quad (16)$$

$$\sigma_\varphi = \frac{\rho\Omega^2}{8} [R_o^2 (3 + \nu) - r^2 (1 + 3\nu)] - \frac{\rho\Omega^2 R_i^2 (1-\nu) [R_o^2 (3+\nu) - R_i^2 (1+\nu)]}{8 [R_i^2 (1-\nu) + R_o^2 (1+\nu)]} \left(\frac{R_o^2}{r^2} + 1 \right) \quad (17)$$

The stress distributions on the rotating disk with free-free boundary conditions are given in the equations below:

$$\sigma_r = \frac{3+\nu}{8r^2} \rho\Omega^2 [(R_i^2 - r^2)(r^2 - R_o^2)] \quad (18)$$

$$\sigma_\varphi = \frac{3+\nu}{8r^2} \rho\Omega^2 [r^2 (R_i^2 + R_o^2) + R_i^2 R_o^2] - \frac{1+3\nu}{8} \rho\Omega^2 r^2 \quad (19)$$

The stress distributions in a rotating disk with free at inner and clamped at outer circumferences are given in the following equation.

$$\sigma_r = \frac{3+\nu}{8} \rho\Omega^2 (R_i^2 - r^2) - \frac{\rho\Omega^2 (1-\nu) [(3+\nu)R_i^2 - (1+\nu)R_o^2] R_o^2}{8 [(1+\nu)R_i^2 + (1-\nu)R_o^2]} \left[1 - \frac{R_i^2}{r^2} \right] \quad (20)$$

$$\sigma_\varphi = \frac{\rho\Omega^2 [(3+\nu)R_i^2 - (1+3\nu)r^2]}{8} - \frac{\rho\Omega^2 (1-\nu) [(3+\nu)R_i^2 - (1+\nu)R_o^2] R_o^2}{8 [(1+\nu)R_i^2 + (1-\nu)R_o^2]} \left[1 + \frac{R_i^2}{r^2} \right] \quad (21)$$

For both clamped inner and outer circumferences, respectively;

$$w(R_i) = 0; \quad w(R_o) = 0; \quad \frac{\partial w}{\partial r} \Big|_{r=R_i} = 0; \quad \frac{\partial w}{\partial r} \Big|_{r=R_o} = 0 \quad (22)$$

For both free inner and outer circumferences, respectively;

$$m_r|_{r=R_i} = 0; \quad m_r|_{r=R_o} = 0; \quad V_r|_{r=R_i} = 0; \quad V_r|_{r=R_o} = 0 \quad (23)$$

and the normalizing constraint is given for each boundary conditions, clamped-clamped, clamped-free, free-free and free-clamped boundary conditions, respectively, below;

$$R_{mn} \left(\frac{R_i + R_o}{m+2} \right) = 1; \quad R_{mn}(R_o) = 1; \quad R_{mn}(R_i) = 1; \quad R_{mn}(R_i) = 1 \quad (24)$$

The boundary conditions and normalizing constraint give a linear system of equations in terms of $X_{mn}^1, X_{mn}^2, X_{mn}^3, X_{mn}^4$ and X_{mn}^5 . The number of linear system of equations for each m and n , is 5 and the unknown coefficients are obtained from the equations of $5(M+1)(N+1)$. Then, the natural frequencies are obtained from Equation (12).

3. RESULTS AND DISCUSSION

In order to validate the solution method, the natural frequencies of a commercially available hard disk are to be calculated. The inner and outer diameters of the hard disk are 32.5 mm and 95 mm respectively and the thickness of the disk is 1.3 mm. Natural frequencies calculated for the hard disk with clamped at inner and free at outer circumferences are given in Table I for $m=0$. Here the abbreviations FTW and BTW stand for forward travelling wave and backward travelling wave, respectively. It should be noted that there is only one natural frequency for $n=0$, while two frequencies are obtained for other n values. Since there is no nodal diameter in the $n=0$ mode, there will be no forward or backward traveling wave. For this reason, except for this mode, two frequency values of each mode are obtained at each rotation speed value.

The results are compared with the experimental and finite element analysis (FEA) results presented in [11]. It can be seen from Table I that the analytical and numerical results are in excellent agreement, for all rotation speeds, with the experimental results. Experimental results of the mode $m=0$, $n=0$ for each rotation speed are higher than those of this study and numerical approach in [11], while the frequency of mode $m=0$, $n=1$ is lower than those of this study and numerical approach in [11]. This may be due to the driving system rigidity. The rigidity of the driving system affects the first and second frequencies of the hard disk. This may cause the frequencies of the mode $m=0$, $n=0$ to rise while those of the mode $m=0$, $n=1$ to fall. As it can be seen from Table I, all other frequencies are in excellent agreement with those of this study and numerical approach in [11].

Table I. Natural frequencies for clamped-free boundary condition and $m=0$.

Rotation speed [rpm]		Wave type	$m=0$				
			$n=0$ [Hz]	$n=1$ [Hz]	$n=2$ [Hz]	$n=3$ [Hz]	$n=4$ [Hz]
0	This Study	-	1052.17	1044.77	1218.80	1890.44	3056.19
	[11] Num.		1050.37	1041.47	1211.47	1878.12	3035.22
	[11] Exp.		1136.00	955.00	1232.00	1830.00	3009.00
4000	This Study	FTW	1055.11	1114.92	1356.45	2094.63	3326.61
	[11] Num.		1053.32	1111.62	1349.14	2082.33	3305.67
	[11] Exp.		1148.00	1009.00	1350.00	2032.00	3276.00
	This Study	BTW	1055.11	981.58	1089.78	1694.63	2793.27
	[11] Num.		1053.32	978.28	1082.48	1682.33	2772.33
	[11] Exp.		1148.00	880.00	1101.00	1641.00	2741.00
8000	This Study	FTW	1063.89	1191.96	1502.65	2307.15	3604.51
	[11] Num.		1062.10	1188.67	1495.40	2294.92	3583.62
	[11] Exp.		1160.00	1077.00	1484.00	2245.00	3553.00
	This Study	BTW	1063.89	925.29	969.31	1507.15	2537.84
	[11] Num.		1062.10	922.01	962.06	1494.92	2516.96
	[11] Exp.		1160.00	820.00	971.00	1454.00	2500.00

Also, in the work by Bashmal et al. [12], the measured natural frequencies are 7.68 kHz and 7.73 kHz for an aluminum disk with an inner diameter of 0.02 m and an outer diameter of 0.15 m at a rotation speed of 1920 rpm. In order to assess the validity of the method, natural frequencies are calculated for the same geometry and material properties in this study as 8290.9 Hz (error: -%7.94) and 8354.9 Hz (error: -%8.07). The results are in acceptable limits.

Table II presents the results of this study for the modes $m=1$, $n=0, 1, 2, 3, 4$. It is obvious that the frequencies calculated are considerably higher than the frequencies presented in Table I.

Table II. Natural frequencies for clamped-free boundary condition and $m=1$.

Rotation speed [rpm]	Wave type	$m=1$				
		$n=0$ [Hz]	$n=1$ [Hz]	$n=2$ [Hz]	$n=3$ [Hz]	$n=4$ [Hz]
0	-	6755.93	7020.41	7839.05	9264.35	11330.75
4000	FTW	6759.11	7090.28	7975.64	9467.66	11600.73
	BTW	6759.11	6956.94	7708.97	9067.66	11067.40
8000	FTW	6768.63	7166.54	8118.74	9677.57	11877.35
	BTW	6768.63	6899.88	7585.41	8877.57	10810.68

Figures 2 and 3 present the natural frequencies of this study and [11] versus the rotation speed of the disk, which is also known as Campbell diagram. It can be seen from Figure 2 that the results of this study and numerical approach given in [11] are in excellent agreement, while the experimental results are about 10% different than those of this study and numerical approach given in [11]. The rigidity of the driving system may cause this difference.

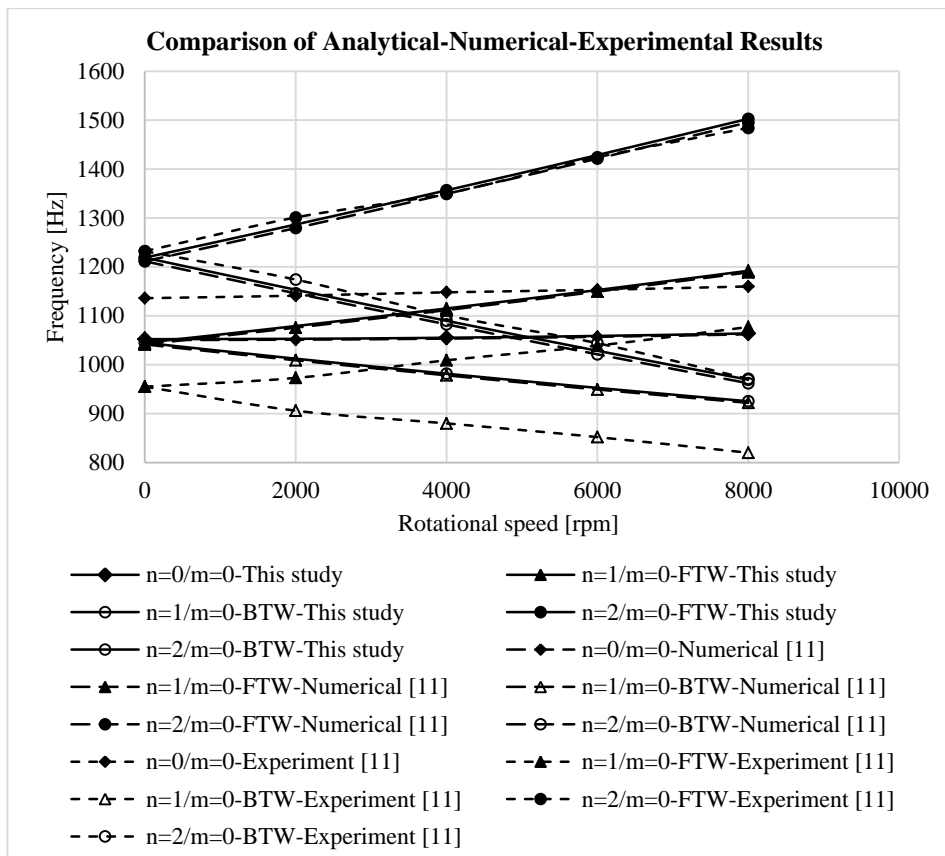


Figure 2. The Campbell diagram of the clamped-free rotating disk for $m=0$ and $n=0, 1, 2$.

As it can be seen from Figure 3, the frequencies of this study and numerical approach given in [11] for all other modes are in excellent agreement with the experimental results in [11].

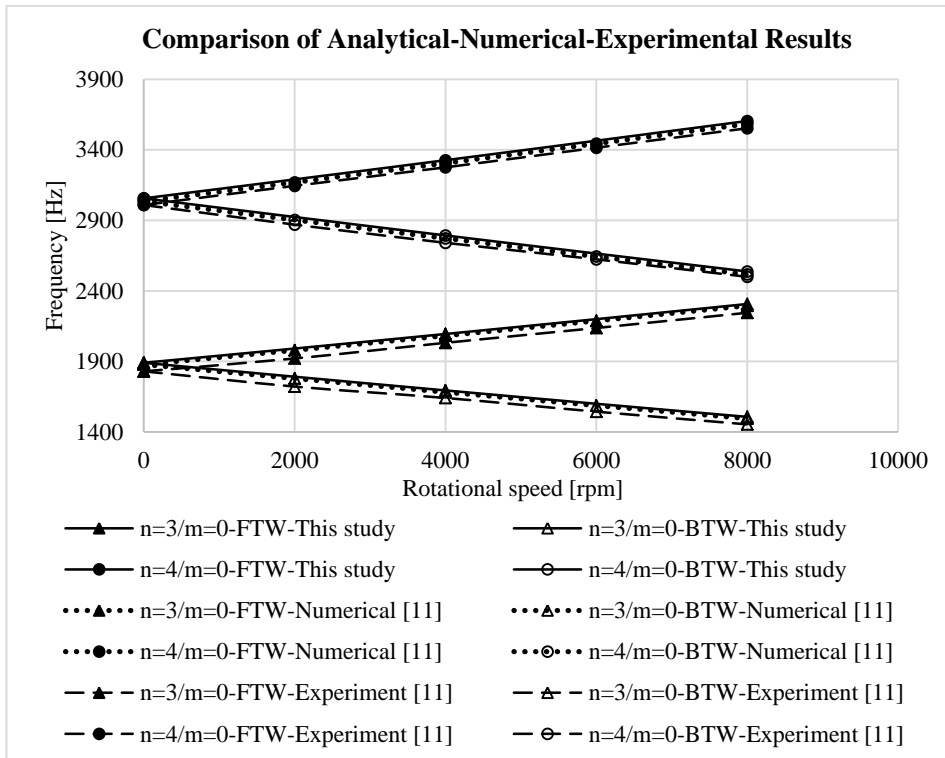


Figure 3. The Campbell diagram of the clamped-free rotating disk for $m=0$ and $n=3, 4$.

The same geometry and material properties given in [11] are used to calculate the natural frequencies of the rotating disks with different boundary conditions. The natural frequencies of the rotating disk with clamped-clamped boundary condition are given in Table III and IV. As it can be seen from Table III and IV, the results are considerably higher than those obtained for the clamped-free disk, as it is expected. The main reason for this difference between the natural frequencies is the boundary conditions. Clamped-clamped boundary conditions cause a stiffer behavior.

Table III. Analytically calculated natural frequencies of the clamped-clamped boundary conditions for $m=0$.

Rotation speed [rpm]	Wave type	$m=0$				
		$n=0$ [Hz]	$n=1$ [Hz]	$n=2$ [Hz]	$n=3$ [Hz]	$n=4$ [Hz]
0	-	7150.87	7320.71	7893.05	9005.47	10760.38
4000	FTW	7151.07	7387.60	8026.68	9205.83	11027.44
	BTW	7151.07	7254.26	7760.01	8805.83	10494.11
8000	FTW	7151.67	7454.94	8160.89	9406.90	11295.29
	BTW	7151.67	7188.28	7627.55	8606.90	10228.63

The natural frequencies of free-clamped rotating disk are also given in Table V and VI. Table V displays the natural frequencies for $m=0$ and $n=0, 1, 2, 3, 4$ and Table VI shows the natural

frequencies for the modes $m=1$ and $n=0, 1, 2, 3, 4$. The results are higher than those of the disk with clamped-free boundary conditions. This could be explained with the length of fixed circumference. Clamped-free boundary conditions have shorter clamped circumference than that of free-clamped disk. Therefore, the stiffer behavior is to be expected. It is interesting to note that the frequencies for $n=0$ decreases with the increasing rotation speed (Table V and VI). Since the stress distribution caused by the rotation throughout the disk is compression, the frequencies decrease slightly when the rotation speed increases.

Table IV. Analytically calculated natural frequencies of the clamped-clamped boundary conditions for $m=1$.

Rotation speed [rpm]	Wave type	$m=1$				
		$n=0$ [Hz]	$n=1$ [Hz]	$n=2$ [Hz]	$n=3$ [Hz]	$n=4$ [Hz]
0	-	19761.65	20019.29	20814.76	22206.89	24268.68
4000	FTW	19761.85	20086.16	20948.32	22407.15	24535.65
	BTW	19761.85	19952.83	20681.66	22007.15	24002.32
8000	FTW	19762.45	20153.46	21082.35	22607.95	24803.23
	BTW	19762.45	19886.79	20549.02	21807.95	23736.56

Table V. Analytically calculated natural frequencies of free-clamped boundary conditions for $m=0$.

Rotation speed [rpm]	Wave type	$m=0$				
		$n=0$ [Hz]	$n=1$ [Hz]	$n=2$ [Hz]	$n=3$ [Hz]	$n=4$ [Hz]
0	-	1679.91	2667.67	4448.18	6706.77	9424.54
4000	FTW	1679.03	2734.18	4581.89	6907.28	9691.21
	BTW	1679.03	2600.84	4315.22	6507.28	9158.28
8000	FTW	1676.39	2800.38	4716.36	7108.79	9959.50
	BTW	1676.39	2533.71	4183.02	6308.79	8892.83

Table VI. Analytically calculated natural frequencies of free-clamped boundary conditions for $m=1$.

Rotation speed [rpm]	Wave type	$m=1$				
		$n=0$ [Hz]	$n=1$ [Hz]	$n=2$ [Hz]	$n=3$ [Hz]	$n=4$ [Hz]
0	-	7932.72	8817.06	11125.77	14324.42	18259.52
4000	FTW	7931.95	8883.14	11258.91	14524.62	18526.64
	BTW	7931.95	8749.80	10992.24	14124.62	17993.30
8000	FTW	7929.63	8948.04	11391.68	14725.20	18794.64
	BTW	7929.63	8681.37	10858.35	13925.20	17727.98

Table VII and VIII present the natural frequencies of the rotating disk with free-free boundary conditions for $m=0, n=0, 1, 2, 3, 4$ and $m=1, n=0, 1, 2, 3, 4$ respectively. As it can be seen from Table VII, the modes $m=0, n=0$ and $m=0, n=1$ are the rigid body modes for a non-rotating disk with free-free boundary conditions. For the mode $m=0, n=0$, the frequencies for all rotation speeds are equal to zero, while the frequencies are small for the mode $m=0$ and $n=1$. For this mode shape, the frequency is zero for the stationary case, while the frequencies are small for all rotation speed.

Table VII. Analytically calculated natural frequencies obtained analytically for free-free boundary conditions.

Rotation speed [rpm]	Wave type	$m=0$				
		$n=0$ [Hz]	$n=1$ [Hz]	$n=2$ [Hz]	$n=3$ [Hz]	$n=4$ [Hz]
0	-	0	0	654.43	1663.49	2975.62
4000	FTW	0	133.33	797.72	1870.78	3248.63
	BTW	0	0	531.05	1470.78	2715.29
8000	FTW	0	266.66	960.06	2092.43	3534.22
	BTW	0	0	426.72	1292.43	2467.55

Table VIII. Analytically calculated natural frequencies obtained analytically for free-free boundary conditions.

Rotation speed [rpm]	Wave type	$m=1$				
		$n=0$ [Hz]	$n=1$ [Hz]	$n=2$ [Hz]	$n=3$ [Hz]	$n=4$ [Hz]
0	-	1164.09	2447.73	4484.42	6958.46	9915.65
4000	FTW	1170.71	2519.54	4623.50	7164.59	10188.35
	BTW	1170.71	2386.21	4356.84	6764.59	9655.02
8000	FTW	1190.36	2601.58	4774.04	7382.94	10473.10
	BTW	1190.36	2334.91	4240.71	6582.94	9406.44

At this stage of the study, the natural frequencies of the disks with different boundary conditions are calculated for the rotation speed up to 30000 rpm and the diagrams of the frequencies are plotted versus the rotation speed.

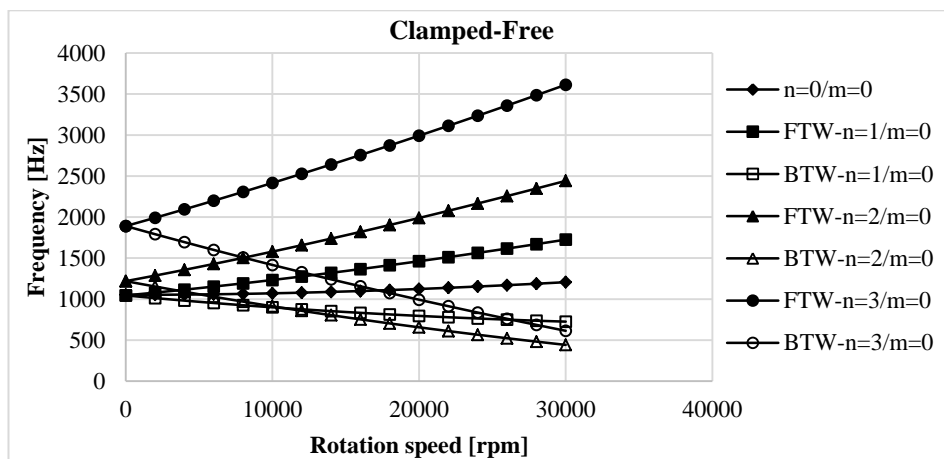


Figure 5. Campbell diagram of clamped-free disk for $m=0$ and $n=0, 1, 2, 3$

Figures 5 and 6 presents the change of the natural frequencies of a clamped-free disk against the rotation speed. As it is presented in Figure 2, the natural frequencies for the mode $m=0, n=0$ increase slightly with the increasing the rotation speed. As it is expected, all the modes except for $n=0$ have two different natural frequencies, forward and backward travelling waves. The natural frequency of the stationary disk for the mode $m=0, n=0$ is slightly higher than that of the mode

$m=0, n=1$. For larger n values, the differences between the natural frequencies of the stationary disk become larger. It is obvious that the frequencies for higher modes become more important for the resonance, if the disk rotates at very high speed. Natural frequencies of the BTW for $n \neq 0$ decrease until zero with the decreasing rotation speed. This rotation speed is called a “critical speed”. Any outer effect can easily initiate the resonance in the disk and lead to disk fatigue failure. Then, the frequency increases with the increasing rotation speed. In Figure 6, the Campbell diagram is given for a clamped-free disk for the modes $m=1$ and $n=0, 1, 2, 3$. The natural frequencies are considerably higher than those for the modes $m=0$. The frequency of the stationary disk for the mode $m=1$ and $n=0$ is lower than that for $m=1$ and $n=1$, on the contrary to the modes $m=0, n=0$ and $m=0, n=1$ in Figure 5. For the stationary case, difference between the natural frequencies are higher than those for the modes $m=0$.

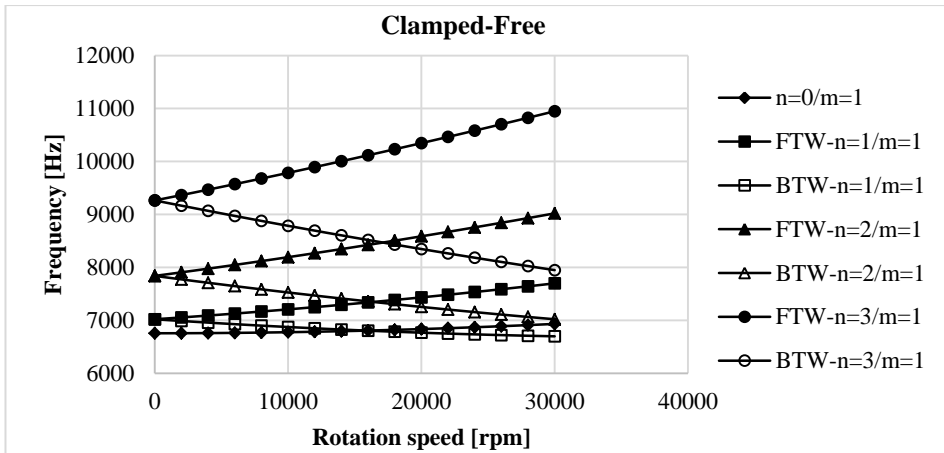


Figure 6. Campbell diagram of clamped-free disk for $m=1$ and $n=0, 1, 2, 3$

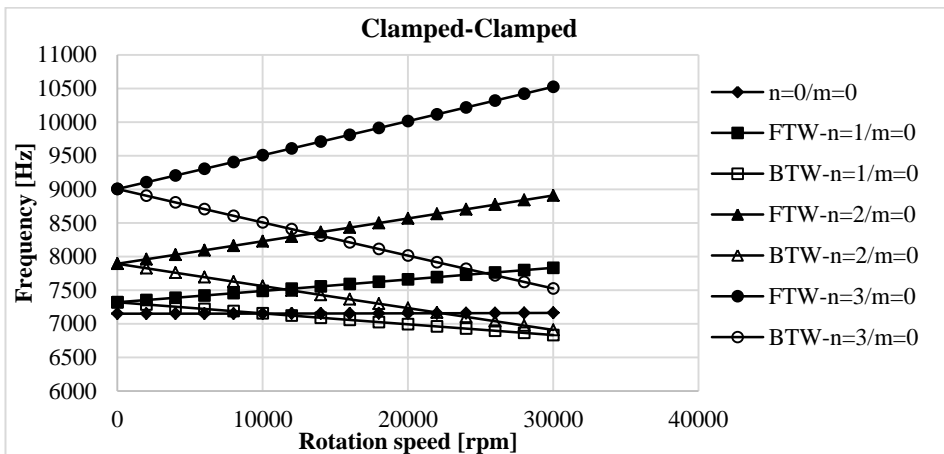


Figure 7. Campbell diagram of a clamped-clamped disk for $m=0$ and $n=0, 1, 2, 3$.

Figure 7 gives the natural frequencies of a disk with clamped-clamped boundary conditions for $n=0, 1, 2, 3$ and $m=0$. Since this type of boundary condition has much higher stiffness than the

clamped-free one, the frequencies are considerably higher than those obtained for the clamped-free boundary condition (See Figure 5). The critical speeds for this boundary condition are considerably higher than those for clamped-free boundary condition. On the contrary to the clamped-free boundary conditions, the frequency of the mode $m=0, n=0$ is lower than that of the mode $m=0, n=1$. The differences between the natural frequencies without rotation are higher than those of the clamped-free boundary conditions.

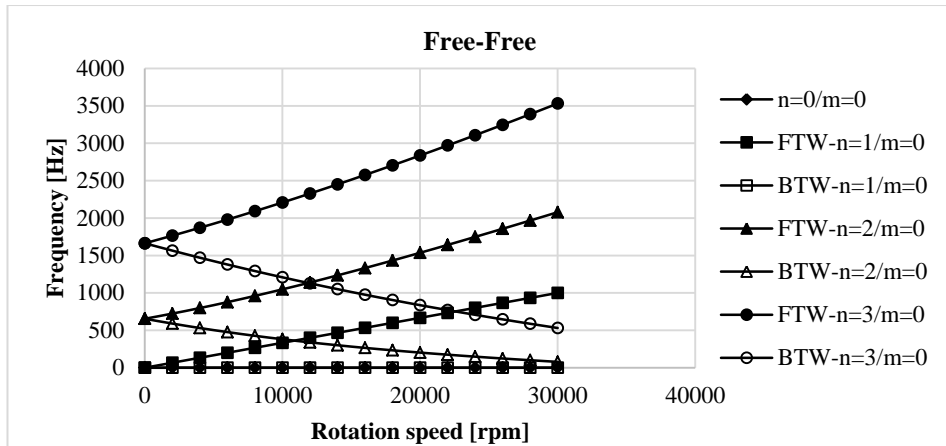


Figure 8. Campbell diagram of free-free disk for $m=0$ and $n=0, 1, 2, 3$

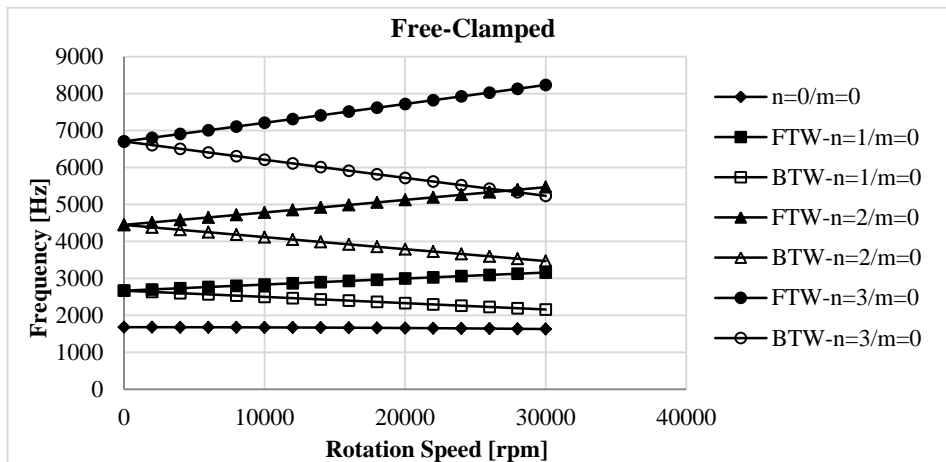


Figure 9. Campbell diagram of free-clamped disk for $m=0$ and $n=0, 1, 2, 3$

Free-free boundary condition is another important case than the clamped-free boundary conditions, since this kind of disks are widely used as splined circular saw blades in the wood cutting machines. The splined circular saw blades are also guided against excessive vibrations. In Figure 8, the natural frequencies of a disk with free-free boundary condition for $m=0$ and $n=0, 1, 2, 3$ are plotted versus the rotation speed. The frequencies are considerably lower than those of the disk with clamped-free boundary conditions, since this boundary conditions cause much less rigidity than that of the clamped-free boundary conditions. Also the differences between the

natural frequencies for stationary case are noticeably larger. All of modes of $m=0$, $n=0$ and the stationary case of $m=0$, $n=1$ are the rigid body modes. The rotation speed affects the mode $m=0$, $n=1$, so the frequencies for the forward and backward travelling waves are observed. It can be seen from the figure that the critical speed for the mode $m=0$, $n=2$ is just around the 30000 rpm.

The frequency change of a free-clamped disk with the rotation speed is given in Figure 9. For stationary case, the frequencies of free-clamped disk are considerably higher than those of clamped-free disk. The frequency of the mode $m=0$, $n=0$ decreases slightly with the increasing rotation speed. This is due to the stress distribution caused by the rotation throughout the disk. The stress distribution is compression, contrary to the case for the clamped-free boundary condition. The compression increases when the rotation speed increases. So, the frequency decreases slightly with the increasing rotation speed. The critical rotation speed is much higher than that of clamped-free disk.

4. CONCLUSIONS

In this paper, free transverse vibrations of rotating annular disks with different boundary conditions are investigated analytically. To obtain dynamical response of structure, the Galerkin method is used by proposing a 5th order polynomial as an approximation function.

As boundary conditions, clamped-clamped, free-clamped and free-free cases are also investigated, besides clamped-free boundary condition. The natural frequencies of the rotating disk are calculated from 0 to 3000 rpm and these values are given in tables and plotted versus the rotational speed as Campbell diagrams.

The obtained results of clamped-free boundary conditions are validated with experimental and numerical ones for $m=0$ given in [11]. Also, in order to show their consistency, the analytical, numerical and experimental results are presented together in Campbell diagrams. The natural frequencies of clamped-clamped disk are higher than those for other boundary conditions, due to being much stiffer than the other boundary conditions. Similarly, because of having no constraint, the natural frequencies for free-free case are the lowest ones and under these boundary conditions, rotating disk has rigid body modes which are $m=0$, $n=0$ for all rotational speeds and mode $m=0$, $n=1$ for stationary case. For free-clamped case, natural frequencies of mode $m=0$, $n=0$, which is known as umbrella mode and does not have any nodal diameter, decrease due to rotation induced compressive stress. When compressive stress increases, the natural frequencies decreases, as it is expected.

REFERENCES

- [1] Lamb H., Southwell R. V., (1921) The Vibrations of a Spinning Disk, *Proceedings of the Royal Society, Series A*, vol. 99, pp. 272-280.
- [2] Southwell R. V., (1921) On The Free Transverse Vibrations of a Uniform Circular Disk Clamped at Its Center, And On the Effects of Rotation, *Proceeding of the Royal Society, Series A*, vol. 101, p. 133.
- [3] Nowinski J. L., (1964) Nonlinear Transverse Vibrations of a Spinning Disk, *Journal of Applied Mechanics*, Vol. 31, Trans. ASME, Vol. 86, Series E, pp. 72-78.
- [4] Mote C. D., (1965) Free Vibration of Initially Stressed Circular Disc, Trans. ASME, *Journal of Engineering for Industry*, May, pp. 258-264.
- [5] Ramaiah G. K., (1981) Natural Frequencies of Spinning Annular Plates, *Journal of Sound and Vibration*, Volume 74, Issue 2, pp. 303-310.
- [6] Bashmal S., (2009) In-Plane Free Vibration of Circular Annular Disks, *Journal of Sound and Vibration*, Vol. 322, pp. 216–226.
- [7] Koo K. N., (2006) Vibration Analysis and Critical Speeds of Polar Orthotropic Annular Disks In Rotation, *Composite Structures*, Vol. 76, pp 67-72.

- [8] Pei Y. C., Tan Q. C., (2009) Modal Interactions of Rotating Flexible Disc, *Proc. ImechE, Part C: J. Mechanical Engineering Science*, vol. 223, no. 4, pp. 851-857.
- [9] Mignolet M. P., Eick C. D., Harish M. V., (1996) Free Vibration of Flexible Rotating Disks, *Journal of Sound and Vibration*, vol. 196, no. 5, pp. 537-577.
- [10] Nayfeh A. H., Jilani A., Manzione P., (2001) Transverse Vibrations of a Centrally Clamped Rotating Circular Disk, *Nonlinear Dynamics*, vol. 26, pp. 163–178.
- [11] Tufekci M., Genel O. E., Oldac O., (2017) Finite Element and Experimental Analysis of Vibrations of a Rotating Disc, *Tokyo 18th International Conference on "Engineering & Technology, Computer, Basic & Applied Sciences" (ECBA- 2017)*, July 25-26, Tokyo, Japan.
- [12] Bashmal S., Bhat R., Rakheja S., (2016) Experimental and Numerical Study of the Vibration of Stationary and Rotating Annular Disks," *Journal of Vibration and Acoustics*, vol. 138 pp. 051003-1-11.